Building and Environment, Vol. 25, No. 2, pp. 155–161, 1990.
Printed in Great Britain.

0360–1323/90 $3.00+0.00

Transfer Rates in Single-Sided Ventilation

M. R. MOKHTARZADEH-DEHGHAN*
M. M. M. EL TELBANY†
A. J. REYNOLDS*

This paper describes a numerical study of the transfer rates associated with single-sided ventilation. It discusses the relationship between the heat transfer rate across the plane of the window opening and the mean temperature maintained in the room. The room is represented by a rectangular two-dimensional cavity which is exposed to the external flow from one side only. Partially closed cavities are studied, to simulate the window effect. The study also describes the effect of the area of heat release on the cavity walls. It is argued that, by analogy between heat and mass transfer, the results are applicable to the transfer rates of the contaminants released in the room.

The mathematical model consists of the governing differential equations of continuity, momentum and energy which, together with two equations for the k–ε *model of turbulence, are solved using a control-volume technique.*

NOMENCLATURE

A_0	window area, m^2
$c_\mu, c_1, c_2, c_3, c_D$	constants in the k–ε turbulent-flow model
c_p	specific heat, J kg^{-1} K^{-1}
C	concentration, kmol m^{-3}
g	gravitational acceleration, m s^{-2}
h	heat transfer coefficient, W m^{-2} K^{-1} ($h = \dot{Q}/A_0\Delta T$)
k	turbulence kinetic energy, N m kg^{-1}
L	window length, m
N	mass rate of release of contaminant in the cavity, kmol m^{-2} s^{-1}
p	time-averaged static pressure, N m^{-2}
$\dot{q}_w$	wall heat flux, W m^{-2}
$\dot{Q}$	heat transfer rate, W
R	gas constant, J kg^{-1} K^{-1}
Re	Reynolds number
S_ϕ	source term for variable ϕ
St	Stanton number
St_c	mass transfer Stanton number
S_T	source term in the energy equation
T	temperature, °C
T_0	outer stream temperature, °C
T_w	wall temperature, °C
T_P	temperature at node P next to wall, °C
T_m	mean temperature in the cavity, °C
u, v	time averaged velocity component, m s^{-1}
U	outer stream velocity, m s^{-1}
u^+	non-dimensional velocity ($u^+ = u/u_\tau$)
u_τ	friction velocity ($u_\tau = \sqrt{\tau_w/\rho}$)
x, y	Cartesian co-ordinates
y^+	non-dimensional distance from the wall ($y^+ = yu_\tau/\nu$)

Greek symbols

β	coefficient of thermal expansion, K^{-1}
Γ_ϕ	diffusion coefficient for variable ϕ ($\Gamma_\phi = \mu/\sigma_\phi$)
ε	rate of dissipation of k, N m kg^{-1} s^{-1}
μ	dynamic viscosity, kg m^{-1} s^{-1}
μ_t	turbulent viscosity, kg m^{-1} s^{-1}
μ_{eff}	effective viscosity, $\mu_{eff} = \mu + \mu_t$
ρ	fluid density, kg m^{-3}
ν	kinematic viscosity, m^2 s^{-1}
ϕ	general dependent variable
$\sigma_T, \sigma_{T,t}$	laminar and turbulent Prandtl numbers, respectively
$\sigma_\varepsilon, \sigma_k$	constants in the turbulence model
τ_w	wall shear-stress, N m^{-2}

Subscripts

1, 2, 3	refer to the heated walls (see Fig. 1)
ref	reference value
P	refer to node P next to wall.

* Department of Mechanical Engineering, Brunel University, Uxbridge, Middlesex, England.
† Faculty of Engineering and Technology, Helwan University, El-Mattaria, Cairo, Egypt.

1. INTRODUCTION

SINGLE-SIDED ventilation is that generated by the wind external to a building, as the wind flows past an opening or openings on one side of the room. Thus the removal of heat or some contaminant from the room is achieved entirely by scavenging processes at the window opening, and not by a bulk flow through the room. The temperature level within the room, or concentration of the contaminant, is achieved by the zero-sum interchange of air which takes place at the window.

It is well known that the transfer processes for fluid–contaminant combinations characterized by molecular Prandtl and Schmidt numbers close to unity are closely analogous to the momentum-transfer processes. This analogy, known as Reynolds analogy, is commonly adopted to relate the transfer of heat, mass and momentum in gases, where the condition is commonly satisfied. In two earlier papers [1, 2], the present authors have investigated in some detail the flow fields associated with single-sided ventilation. The study was based on hot-wire measurements, flow visualization and also a mathematical model. The factors included in these studies were: cavity (or room) shape, the influence of acceleration and deceleration of the outer flow, Reynolds number of

the flow, and size and location of the opening (or window) between internal and external flows.

There are a number of studies in the literature which deal with the fluid flow and heat transfer in fully-open cavities [3–5]. Humphrey and To [3] have carried out a detailed numerical study (based on the k–ε model) of free and forced convection flows in a heated two-dimensional cavity of arbitrary inclination to the gravity direction. They have discussed some of the most relevant studies on the subject and have given a number of correlations relating Nusselt and Stanton numbers to the Reynolds and Grashof numbers.

The studies by Yamamoto *et al.* [4] and Ideriah [5], not cited by Humphrey and To [3], are also relevant to the present work. Yamamoto *et al.* [4] have studied experimentally the forced convection heat transfer from heated cavities of various depth to width ratios. They have also given correlations for the Nusselt number in terms of the Reynolds number and the depth to width ratio. Ideriah [5] has carried out a numerical study of turbulent flow in a heated cavity driven by the external flow in an adjoining channel. He adopted the same numerical method and the turbulence model as have been adopted in the present study. The results for the fluid flow and temperature fields are given for Reynolds numbers mainly in the range of 10 000 to 200 000 and Archimedes numbers ($Ar = Gr/Re^2$) between 0 and 0.37. However, the height of the adjoining channel, containing the "external" flow, was relatively small compared with the cavity depth. Since this configuration is likely to modify significantly the development and location of the shear layer, the results are of limited application to building ventilation.

The present paper addresses the problem of specifying the transfer between internal and external flows, and thus the internal temperature (or concentration) level. The contaminant considered is in fact thermal energy, and the concentration is thus measured by the temperature level in the room. The investigation is based on computer modelling, using the same mathematical model as the earlier studies [1, 2]. The approach is justified by the detailed comparisons made in the earlier papers between measurement, flow visualization and results of computation.

The particular contributions of this study which distinguish it from earlier studies are:

- Consideration of partially open cavities, representative of more normal room configurations where the window occupies only part of the "open" wall
- Consideration of a number of heating modes, in an attempt to develop results that are more-or-less independent of the way in which heat is released within the "room"
- The use of a mean air temperature (in determining the temperature level above that of the external flow), rather than a wall temperature (as adopted by other investigators), in order to produce results representative of in-room conditions
- Concentration on higher values of Reynolds number, where effects of buoyancy are insignificant
- Extension of the results to transfer of passive contaminants.

2. THE MATHEMATICAL MODEL

The governing differential equations of mass, momentum and thermal energy can be written in the following general form:

$$\frac{\partial}{\partial x}(\rho u\phi) + \frac{\partial}{\partial y}(\rho v\phi) = \frac{\partial}{\partial x}\left(\Gamma_\phi \frac{\partial \phi}{\partial x}\right) + \frac{\partial}{\partial y}\left(\Gamma_\phi \frac{\partial \phi}{\partial y}\right) + S_\phi, \tag{1}$$

where $\phi = 1$, u, v or, T. The diffusion coefficients Γ_ϕ and the source terms S_ϕ are given in Table 1. The turbulence model adopted in this study is the k–ε model. As a result, two additional equations, one for the turbulence energy k and the other for its rate of dissipation ε, are solved simultaneously with the other equations. These two equations are also written in the form of equation (1), using the substitutions shown in Table 1. The eddy viscosity is then calculated from k and ε using the relationship (T.1) in Table 1. A detailed description of the k–ε model and other turbulence models can be found in [6]. The set of governing differential equations are transformed into discretised forms using a control-volume method. These are then solved using the Line-by-Line method and TDMA (Tri-Diagonal Matrix Algorithm [7]). The solution procedure employs the SIMPLE (Semi-Implicit Method for Pressure-Linked Equations) method of Patankar and Spalding [8] for calculation of pressure. Full details of these procedures can be found in [7].

The buoyancy terms in the v-momentum, k and ε equations are given here for completeness. In fact, in the present study the effect of buoyancy forces is small. This can be realized with reference to the values of the parameter Re^2/Gr, which denotes the ratio of inertia forces to buoyancy forces. Humphrey and To [3] have concluded that for $Re^2/Gr > 2$ the heat loss from a cavity is strongly affected by the inertia forces. For $Re^2/Gr > 21.3$ the flow field in the cavity is dominated by the inertia forces and becomes independent of orientation of the cavity. For the range of parameters adopted in the present study (see Table 2) the buoyancy forces are therefore negligible.

The special treatment of the flow near walls follows the well-known wall-function method [4, 9]. According to this method, the heat flux from a wall, which is kept at a constant temperature T_w, to the turbulent flow adjacent to it is calculated from:

$$\dot{q}_w = \frac{\rho c_p c_\mu^{1/4} k_P^{1/2}(T_w - T_p)}{T_P^+}, \tag{2}$$

which is derived using the relations for turbulent boundary layers as explained in [6]. T_P^+ is defined as:

$$T_P^+ = \sigma_{T,t}[u_P^+ + f]. \tag{3}$$

The function f can take different forms. The one which is used in this study is due to Jayatillaka [10], given by:

$$f = 9.24\left[\left(\frac{\sigma_T}{\sigma_{T,t}}\right)^{3/4} - 1\right]\left[1 + 0.28\exp\left(-0.007\frac{\sigma_T}{\sigma_{T,t}}\right)\right]. \tag{4}$$

T_p in equation (2) is the temperature at a node on the first grid line adjacent to the wall. Equation (2) implies that the first grid line should therefore be located in

Table 1. The differential equations of the mathematical model

Equation	ϕ	Γ_ϕ	S_ϕ
Continuity	1	0	
u-momentum	u	μ_{eff}	$-\frac{\partial p}{\partial x}+\frac{\partial}{\partial x}\left(\mu_{\text{eff}}\frac{\partial u}{\partial x}\right)+\frac{\partial}{\partial y}\left(\mu_{\text{eff}}\frac{\partial v}{\partial x}\right)$
v-momentum	v	μ_{eff}	$-\frac{\partial p}{\partial y}+\frac{\partial}{\partial x}\left(\mu_{\text{eff}}\frac{\partial u}{\partial y}\right)+\frac{\partial}{\partial y}\left(\mu_{\text{eff}}\frac{\partial v}{\partial y}\right)-g(\rho-\rho_{\text{ref}})$
Turbulence energy	k	$\mu_{\text{eff}}/\sigma_k$	$G_k-C_D\rho\varepsilon+\rho g\beta\overline{v'T'}$
Energy dissipation	ε	$\mu_{\text{eff}}/\sigma_\varepsilon$	$C_1\frac{\varepsilon}{k}G_k-C_2\rho\frac{\varepsilon^2}{k}+C_3\rho\frac{\varepsilon}{k}g\beta\overline{v'T'}$
Energy equation	T	Γ_{eff}	S_T

$$\Gamma_{\text{eff}}=\frac{\mu}{\sigma_T}+\frac{\mu_t}{\sigma_{T,t}},\quad \mu_t=c_\mu\rho\frac{k^2}{\varepsilon}\text{(T.1)},\quad \mu_{\text{eff}}=\mu+\mu_t,$$

$$-\rho\overline{v'T'}=\Gamma_{T,t}\frac{\partial T}{\partial y},\quad G_k=\mu_t\left[2\left[\left(\frac{\partial u}{\partial x}\right)^2+\left(\frac{\partial v}{\partial y}\right)^2\right]+\left(\frac{\partial u}{\partial y}+\frac{\partial v}{\partial x}\right)^2\right],\quad \rho=\frac{p_{\text{ref}}}{RT}.$$

The empirical constants have been adopted from Launder and Spalding [11] and take the following values: $c_\mu=0.09$, $c_D=1.0$, $c_1=1.44$, $c_2=1.92$, $c_3=1.0$, $\sigma_k=1.0$, $\sigma_\varepsilon=1.3$.

the turbulent region of the boundary layer, say, when $y^+>30$. If the calculations indicate that $y^+<11.63$, then simpler relations describing the heat flux by conduction through the viscous sublayer are used. A full account of the treatment for the flow in the boundary-layer region, and the incorporation of the boundary conditions can be found in [4].

3. GEOMETRY OF THE PHYSICAL DOMAIN

Figure 1 and Table 2 show the geometry of the cavity and the external-flow conditions. The basic square shape is adopted for most calculations, but a cavity whose depth is one half its open width is also considered. In addition to cavities fully open to the external air flow, con-

Table 2. Results for the calculations carried out

Case	L/B	U (m s^{-1})	10^{-5} Re	Heated wall	$\dot{Q}_1$ (W)	$\dot{Q}_2$ (W)	$\dot{Q}_3$ (W)	$\dot{Q}$ (W)	ΔT (°C)	$10^3 h$ (W m^{-2} K^{-1})	10^3 St	Geometry
1	1.0	10	2	1	358	−60	−28	270	6.6	135	11.1	→ 2 3 1
				2	−23	358	−33	302	6.9	144	11.8	
				3	−76	−62	558	420	12	114	9.4	
2	1.0	5	1	1	214	−50	−20	144	6.6	72	12.2	
				2	−16	273	−27	230	7.6	99	16.8	
				3	−52	−50	355	253	13.2	63	10.7	
3	1.0	50	10	1	1272	−156	−79	1037	6.2	553	9.4	
				2	−49	1221	−70	1102	4.7	773	13.1	
				3	−200	−157	1872	1515	9.4	526	8.9	
4	1.0	10	1	1	214	−46	−19	149	6	162	13.7	
				2	−20	241	−26	−195	9.1	140	11.9	
				3	−43	−31	294	220	9.6	151	12.8	
5	1.0	10	1	1	249	−34	−24	191	8.6	146	12.4	
				2	−12	193	−18	163	5.7	186	15.8	
				3	−54	−31	367	282	13.5	138	11.7	
6	1.0	10	1	1	187	−41	−18	128	9.5	89	7.5	
				2	−13	196	−13	170	6.6	170	14.4	
				3	−33	−23	191	135	7.7	115	9.7	
7	1.0	5	1	1	265	−54	−24	187	6.7	91	15.3	The same as case 2 but with uniform inlet velocity
8	0.5	10	2	1	463	−45	−21	397	9.5	137	11.3	→
				2	−11	224	−6	207	3.1	219	18	
				3	−54	−15	333	264	5.9	145	12	

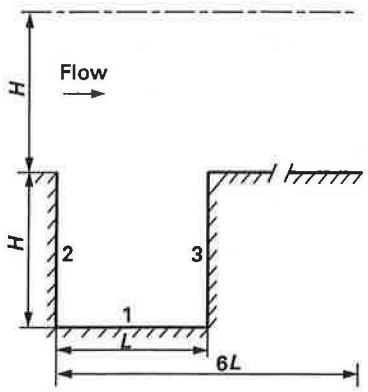

Fig. 1. Schematic diagram of the cavity. $L = H = 0.306$ m.

sideration is also given to half-open cavities (that is, when the opening occupies half the "window" wall) as shown in Table 2.

4. BOUNDARY CONDITIONS

The inlet conditions for velocity and turbulence energy were based on our experimental data and were the same as those adopted in the calculations reported in [1, 2]. The temperature at inlet was set at 19°C. The mainstream velocity was 10 m s^{-1} and the boundary-layer thickness was 27 mm for most of the calculations. However, velocities of 5 m s^{-1} and 50 m s^{-1} have also been considered, giving Reynolds numbers 1×10^5 to 10×10^5, spanning the range between experimental models and realistic rooms.

The north-end of the flow domain was bounded by a symmetry axis as shown in Fig. 1. At the outlet plane, the v-components were set to zero, and the u-components were calculated using the predicted u-values at the upstream plane, so that the overall conservation of mass was satisfied.

One of the inner walls was kept at constant temperature of 100°C. This condition was set in turn at each of the three walls (1, 2 or 3), as identified in Fig. 1. The temperatures of the two other walls were set at 20°C.

5. COMPUTATIONAL DETAILS

The grid was 46×46. In the y-direction, 23 lines were placed in the cavity and the rest between the window and the symmetry axis. The grid lines were more concentrated near the walls and in the shear layer region. In the x-direction, 23 lines were located inside the cavity and the rest in the downstream side.

The Reynolds number used to characterise the flow was defined as:

$$Re = \frac{UL}{\nu}, \tag{5}$$

where U is the imposed uniform outer velocity, and L is the length of the window, measured in the direction of the outer flow.

The heat transfer characteristics of the several shear layers developed in the circumstances defined in Table 2 have been determined in terms of a Stanton number defined as:

$$St = \frac{\dot{Q}}{\rho c_p A_0 U \Delta T}, \tag{6}$$

where $\dot{Q}$ is the heat transfer rate through the "window", between the room and the external flow. It is determined from:

$$\dot{Q} = \dot{Q}_1 + \dot{Q}_2 + \dot{Q}_3, \tag{7}$$

that is, the algebraic sum of the heat transfer rates into or out of the room from the walls, obtained by integration over the three inner faces. A_0 represents the area through which the transfer between the room and the external flow takes place, that is, the window area. ΔT is defined as:

$$\Delta T = T_m - T_0, \tag{8}$$

where T_m represents the mean temperature within the cavity, and T_0 is the imposed outer temperature.

Three different measures of T_m were considered, namely, the temperature at its geometric centre, the temperature averaged over the volume symmetrically disposed about the centre and occupying 50% of the entire enclosed volume, and the temperature averaged over the entire room. As a consequence of the highly effective turbulent mixing in the room, the three differed only slightly, and the second was chosen as best representing typical conditions in the room, away from the heating surface itself.

The same computer program used in our earlier studies [1, 2] was used, so that the results will be directly comparable.

6. RESULTS

Table 2 presents the key results of the calculations carried out. Cases 1–3 demonstrate the results for a fully open square cavity. Each of these cases comprises three sub-cases, for heating of one of the three cavity walls, 1, 2 and 3, respectively. Cases 4–6 represent results for a 50% open cavity, for the same arrangements for the heating of the walls. Case 7 is given to demonstrate the effect of introducing a uniform velocity just upstream of the window, rather than the boundary-layer profile adopted in other calculations. In case 8 a more shallow cavity has been considered.

Inspection of the tabled values leads to the following observations in relation to the variation of the Stanton number:

(a) For the situations considered, almost all the Stanton numbers characterising the transfer processes fall into the range 0.009–0.016. It would be possible, of course, to move beyond these limits by selecting particular combinations of conditions. Nevertheless, it appears that a value around $St = 0.012$ is representative of the shear-layer activity in varied circumstances.

(b) For the fully open cavity, the effect of

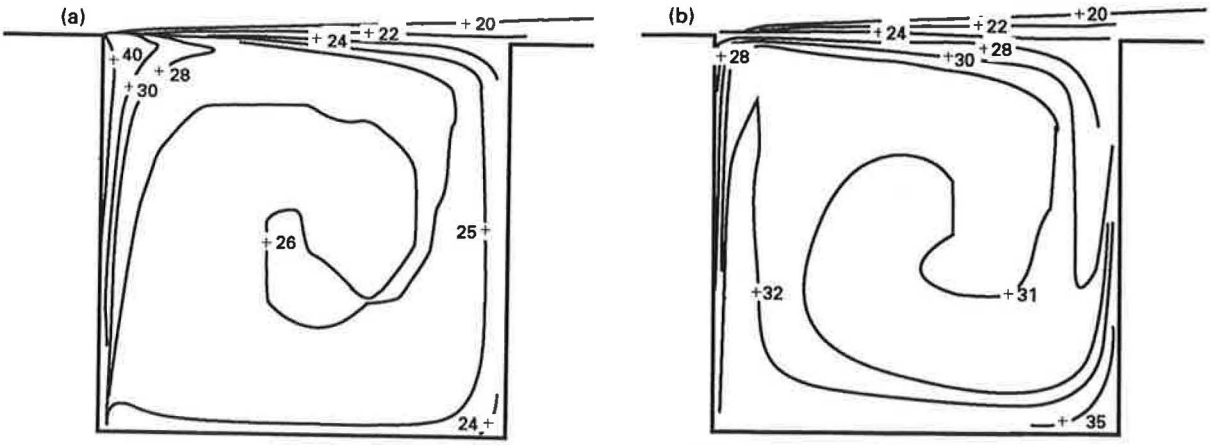

Fig. 2. Contours of temperature in the fully open cavity: (a) Wall 2 is heated; (b) Wall 3 is heated.

Reynolds-number variation is small for the higher values ($Re = 200\,000$ and $1\,000\,000$) representative of modestly-sized models and of actual rooms.

The position of the heating surface within the room gives rise to changes typically between 10 and 25 per cent from the average value. The reason for this is manifest in Figs 2a and b which show, respectively, the temperature contours for cases when walls 2 or 3 are heated. Evidently, in the latter case the heat introduced has a better opportunity to diffuse into the central part of the cavity, and the temperature change across the shear layer is larger.

The heat-transfer rates through all three walls ($\dot{Q}_1$, $\dot{Q}_2$, $\dot{Q}_3$) increases as Reynolds number increases. As a consequence of this, the total heat transfer rate $\dot{Q}$ across the plane of the window increases. The same trend can be seen for the heat-transfer coefficient h, but not for the scaled coefficient St.

(c) The typical effect of reducing the size of the window is modest, the Stanton number changing on average by some 10% when the aperture is changed from fully open to half open. However, the position of the window on the wall is important, with variations of some 20% about the mean being typical as the position is changed. The smallest transfer rates are predicted for a window placed on the upstream side of the room (case 6). Figure 3 shows the contours of temperature for a case of half-open cavity.

(d) The structure of the outer boundary layer is of considerable importance. For the somewhat extreme deviation introduced in these calculations (case 7) a 25% increase in transfer rate is engendered. One must surmise that changes in the external pressure gradient (leading to acceleration or deceleration of the outer flow—not investigated here) will also give rise to significant changes in the transfer rate. In this connection it is worth noting that the structure of the shear layer was found in [1] to depend strongly on the external pressure gradient.

(e) Finally, as would be anticipated, the shape of the room has a marked effect on the transfer rate. For the flatter cavity considered (case 8), the transfer rate is increased and the dependence on the position of heat release within the cavity is stronger (Fig. 4). These trends are what simple geometric considerations would suggest.

7. DISCUSSION

Humphrey and To [3] have developed a simple relationship (for fully-open cavities), applicable to high

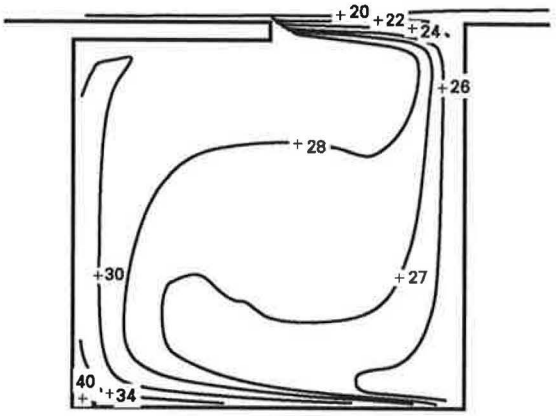

Fig. 3. Contours of temperature in the half-open cavity. Wall 1 is heated.

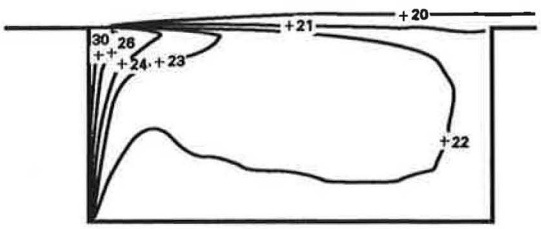

Fig. 4. Contours of temperature in the shallow cavity. Wall 2 is heated.

values of Re^2/Gr, between the Stanton number and the Reynolds number:

$$St = aRe^b, \tag{9}$$

where $a = 0.0154$ and $b = -0.14$. If three ranges for the Reynolds number, namely, (i) 100 000–200 000, (ii) 200 000–1 000 000 and (iii) 100 000–1 000 000 are considered (for each of the three modes of heating, i.e. heated walls 1–3), then forms of equation (9) can be derived from the results given in Table 1, leading to nine values of b ranging from -0.081 to -0.136. Taking a weighted average of these values (namely, weight 1 for range (i), weight 2 for range (ii) and weight 3 for range (iii)) we obtain values of b equal to -0.114, -0.089 and -0.083 for heated walls 1, 2 and 3, respectively. This suggests that a value of b about -0.10 is broadly representative of heat transfer from cavities for varied modes of heat input.

Returning to the results given in Table 2, the computed flow fields suggest that the transfer rate and the temperature are related by $St = 0.012$, typically. This value, allowing for the difference in the definition of ΔT in the present work and that in Humphrey and To [3] (where ΔT has been defined as the difference between the average of the temperatures of the three cavity walls and the temperature of the outer stream) is consistent with the values obtained using equation (9). The results of [1, 2] showed that the measured shear stresses differ by at most 10% from those predicted. Since the air flows under consideration are ones in which a close relationship between momentum and heat transfer is to be expected, one is led to suppose that the transfer rates within the shear layer are also predicted by the computational model with the same accuracy. This justifies the use of the value $St = 0.012$ as a guide in relating heat inputs and air temperatures.

The results given above can be presented more explicitly in the form:

$$\Delta T = \frac{80\dot{Q}}{\rho c_p A_0 U}, \tag{10}$$

which presents the temperature elevation within the room in terms of the net rate of energy release to the flow within the room and other relevant factors. This result can be extended to transfers of a passive contaminant released within the room (for example, water vapour, carbon dioxide or some other product of combustion) by recasting it in terms of the mass-transfer Stanton number:

$$St_c = \frac{N}{U\Delta C}, \tag{11}$$

where N is the mass rate of release of the contaminant, and ΔC is the mass concentration within the cavity. In practical terms, we can write:

$$\Delta C = \frac{80N}{U}. \tag{12}$$

The investigation of sensitivities undertaken earlier in this paper suggests that the simple rules given above are subject to variations as large as 50%, depending on factors such as the way in which the heat (or contaminant) is released, the nature of the outer flow, the size and position of the window, and the shape of the room. By carrying out a systematic programme of calculation, covering perhaps hundred diverse cases, it would be possible to prepare a table from which more accurate values of the characteristic Stanton number might be selected. By this means one might reduce the uncertainty in the prediction of the transfer to perhaps 20%. More precise estimates than these would seem to require computer modelling or measurement of the transfers using specially designed models. An accuracy of perhaps 10% might then be attained.

Although the actual turbulent processes through which momentum and heat (or mass) transfers are achieved are fairly closely analogous, it is a matter of some delicacy to relate the overall shear forces and transfer rates. In flows of the kind considered here, with upstream- and downstream-facing surfaces on which pressure forces are developed, and with significant mean bulk-convection terms, momentum and energy balances are of a complex form, and great care must be taken in determining the quantities characteristic of the flow that can meaningfully be compared. In particular, it is vital to distinguish between transfers across the mean dividing streamline between cavity flow and external flow (where Reynolds analogy might be expected to apply) and the transfers across the closely adjacent plane separating cavity and the external region.

It should be noted that the mechanism of energy and momentum transfer which is considered in this paper is the shear layer which develops spontaneously at the interface separating the room and the external flow, modified in some degree by the boundary layer in the external flow. There is, however, another possible mechanism inducing single-sided ventilation, namely the pumping action of large-scale turbulence, or gustiness, in the flow around the building. This is the phenomenon studied by authors such as Cockroft and Robertson [11].

8. CONCLUSIONS

The calculations reported in this paper provide the means of estimating the transfer rates achievable through single-sided ventilation. The magnitude of the variations associated with changes in parameters defining the system has also been determined. Although these predictions provide the best available basis for design calculations, direct experimental verification of the computed results is desirable.

Acknowledgements—The authors wish to acknowledge the support of the Science and Engineering Research Council, through its "Energy in Buildings" Specially Promoted Programme.

REFERENCES

1. M. M. M. El Telbany, M. R. Mokhtarzadeh-Dehghan and A. J. Reynolds, Single sided ventilation—I. The flow between a cavity and external air stream. *Bldg Envir.* **20**, 15–24 (1985).
2. M. M. M. El Telbany, M. R. Mokhtarzadeh-Dehghan and A. J. Reynolds, Single sided ventilation—II. Further considerations. *Bldg Envir.* **20**, 25–32 (1985).

3. J. A. C. Humphrey and W. M. To, Numerical simulation of buoyant, turbulent flow—II. Free and mixed convection in a heated cavity. *Int. J. Heat Mass Transfer* **29**, 593–610 (1986).
4. H. Yamamoto, N. Seki and S. Fukusako, Forced convection heat transfer on heated bottom surface of a cavity. *J. Heat Transfer* **101**, 475–479 (1979).
5. F. J. K. Ideriah, Prediction of turbulent cavity flow driven by buoyancy and shear. *J. Mech. Engng Sci.* **22**, 287–295 (1980).
6. W. Rodi, *Turbulence Models and their Application in Hydraulics—A State of the Art Review*. International Association for Hydraulic Research, Delft (1980).
7. S. V. Patankar, *Numerical Heat Transfer and Fluid Flow*. McGraw Hill, New York (1980).
8. S. V. Patankar and D. B. Spalding, A calculation procedure for heat, mass and momentum transfer in three dimensional parabolic flows. *Int. J. Heat Mass Transfer* **15**, 1787–1806 (1972).
9. B. E. Launder and D. B. Spalding, Turbulence models and their application to the prediction of internal flows. *Heat Fluid Flow* **21**, 43–54 (1972).
10. C. V. L. Jayatillaka, The influence of Prandtl number and surface roughness on the resistance of the laminar sub-layer to momentum and heat transfer. *Progress in Heat and Mass Transfer. Vol.* 1. Pergamon Press, London (1969).
11. J. P. Cockroft and P. Robertson, Ventilation of an enclosure through a single opening. *Bldg Envir.* **11**, 29–35 (1976).